

Designing Nanostructured Organic-Based Material by Combining Plasma Polymerization and the Wrinkling Approach

Nathan Vinx, David Tromont, Adrien Chauvin, Philippe Leclère, Rony Snyders, and Damien Thiry*



Cite This: <https://doi.org/10.1021/acs.langmuir.3c01873>



Read Online

ACCESS |



Metrics & More

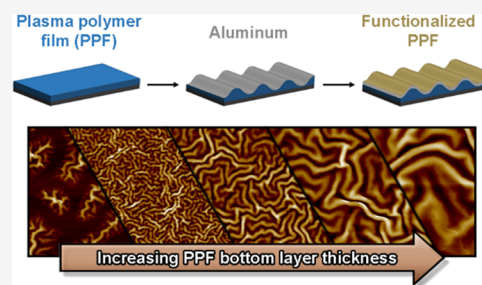


Article Recommendations



Supporting Information

ABSTRACT: In this work, an innovative and versatile strategy for the fabrication of nanostructured organic thin films is established based on the wrinkling phenomenon taking place in a bilayer system constituted by a liquid plasma polymer film (PPF) and a top Al coating. By means of morphological characterization (i.e., atomic force microscopy and scanning electron microscopy), it has been demonstrated that the wrinkle dimensions (i.e., wavelength and amplitude) evolve as a function of the PPF thickness according to models established for conventional polymers. The wrinkled surfaces exhibit great stability over time as their dimension did not vary after 100 days of aging, resulting from a pinning phenomenon between the Al layer and the Si substrate, hence freezing the morphology. In a second step, the wrinkled surfaces have been employed as templates for the deposition of an additional PPF third layer, giving rise to the formation of a nanostructured organic-based surface. The chemical composition of the material can be tuned through an appropriate choice of precursor (i.e., allyl alcohol or propanethiol).



INTRODUCTION

For many years, plasma technologies have been gaining increasing attention for their ability to tune the surface properties of materials by activating the surface or depositing a thin film on it.^{1,2} Among the numerous plasma-based techniques, the plasma polymerization belonging to the PECVD (“plasma enhanced chemical vapor deposition”) family appears particularly attractive to synthesize organic thin polymer films, the so-called plasma polymer films (PPFs).³ Briefly, plasma polymerization consists of the activation of an organic vapor into a plasma phase, resulting in the formation of reactive species (including radicals and to a lesser extent ions), followed by their condensation on surfaces exposed to the discharge. The molecular growth mechanism, comprising a complex interplay between surface and gas phase reactions, triggers the uniqueness of PPF such as the absence of a repeating unit in their polymeric network and the outstanding range of chemical compositions they can exhibit, combined with their thermal stability and their good adhesion properties on all kinds of substrates (i.e., metals, polymers, oxides) for instance.^{4,5} Furthermore, the easiness and the low environmental impact of the process coupled with the long-term economic interests of an investment⁶ makes the plasma polymerization process a reliable technique for surface engineering with a high applicative potential in the biomedical field,^{7,8} for corrosion protection,^{9,10} in electronics,^{11,12} etc. However, nowadays, one of the limiting factors for further developments in the field is the restricted panel of possibilities to produce nanostructured plasma polymers. Indeed, for most of the synthesis conditions, PPF appears smooth and pinhole

free. Nevertheless, structuring the surface of a material at the nanoscale leads to unprecedented physicochemical properties appealing for several technological applications including the control over the material (super)hydrophobicity, the fabrication of highly sensitive biosensors, or in the field of flexible electronics to name a few.^{12–15} To date, nanostructuring methods involving PPF mostly require templates previously manufactured or additional post-treatment processes (e.g., UV, etching, etc.).^{15–20} However, in all cases, the control of the morphology at the nanoscale of the material is extremely limited.

Recently, our group has established a novel and versatile method for the design of a nano/micro pattern with tunable dimensions.^{12,21} The strategy was based on the spontaneous wrinkling phenomenon taking place in bilayer systems consisting of a viscous PPF fluid and a magnetron-sputtered Al layer. If the preliminary results highlighted the attractiveness of our method, several aspects remain unclear regarding the dependence of the wrinkle dimensions on the thickness of the PPF and the stability over time of the nanostructures.

In this context, the first objective of this work is to widen our understanding of the wrinkling phenomenon involving a liquid

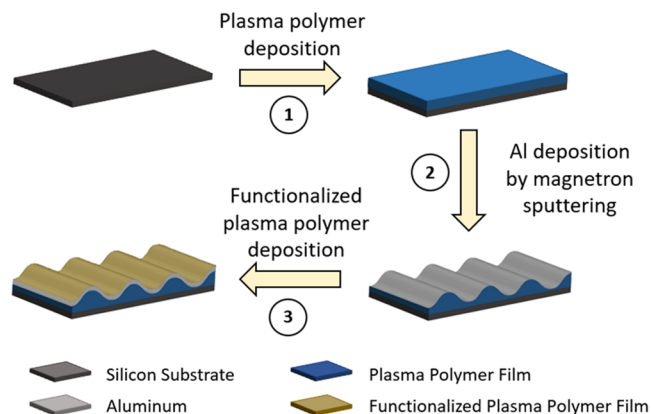
Received: July 6, 2023

Revised: September 26, 2023

plasma polymer and Al coating as compliant and top layers, respectively. In the second step, in view of developing an attractive method for the fabrication of nanostructured PPF (see Scheme 1), the wrinkled structure is employed as a

(i.e., propanethiol and allyl alcohol) are considered for the deposition of the third layer.

Scheme 1. Schematic Description of the Research Strategy Developed in This Study^a



^a(1) Synthesis of a liquid PPF on Si. (2) Deposition of an aluminum coating by magnetron sputtering. (3) Deposition of a functionalized plasma polymer on the PPF/Al bilayer.

pattern for the deposition of an additional PPF taking advantage of the inherent conformal deposition of plasma polymers. To illustrate the flexibility that our strategy offers for controlling in addition to the nanoarchitecture of the material, the surface chemical composition, two different precursors

EXPERIMENTAL SECTION

Substrate Preparation. The depositions of propanethiol-based plasma polymer films have been carried out from 1-propanethiol (99%, Sigma-Aldrich) on 1×1 cm² Silicon wafers. The substrates were cleaned with 1-isopropanol three times and dried under a nitrogen flow before their introduction in the deposition chamber.

Plasma Polymerization. The depositions have been carried out in a metallic vacuum chamber: 65 cm in length and 35 cm in diameter. The reactor was pumped by a combination of turbomolecular and primary pumps leading to a residual pressure lower than 2×10^{-6} Torr. More details about the deposition chamber can be found elsewhere.²² During the depositions, the plasma was sustained by a water-cooled Cu coil (10 cm in diameter). The coil was located inside the chamber at 10 cm from the sample surface and connected to an Advanced Energy radio frequency (13.56 MHz) power supply via a matching network. The depositions were carried out at a constant pressure of 4×10^{-2} Torr controlled by a throttle valve connected to a capacitive gauge. The precursor flow rate was fixed at 10 sccm. Regarding the deposition of the bottom layer, the power applied to the coil was 40 W for all experiments. The substrate temperature was measured during the depositions with a thermocouple affixed to the substrate holder and externally kept constant at 10 ± 1 °C with liquid nitrogen. The choice of these conditions is guided by our previous works.^{12,21} For all experiments, the substrate temperature was fixed 30 min before starting the deposition, ensuring a thermal equilibrium between the substrate holder and the substrate surface.

Regarding the additional plasma polymer deposited on the bilayer system, two precursors are considered: propanethiol (Sigma-Aldrich 99%) or allyl alcohol (Sigma-Aldrich 99%). In both cases, the power

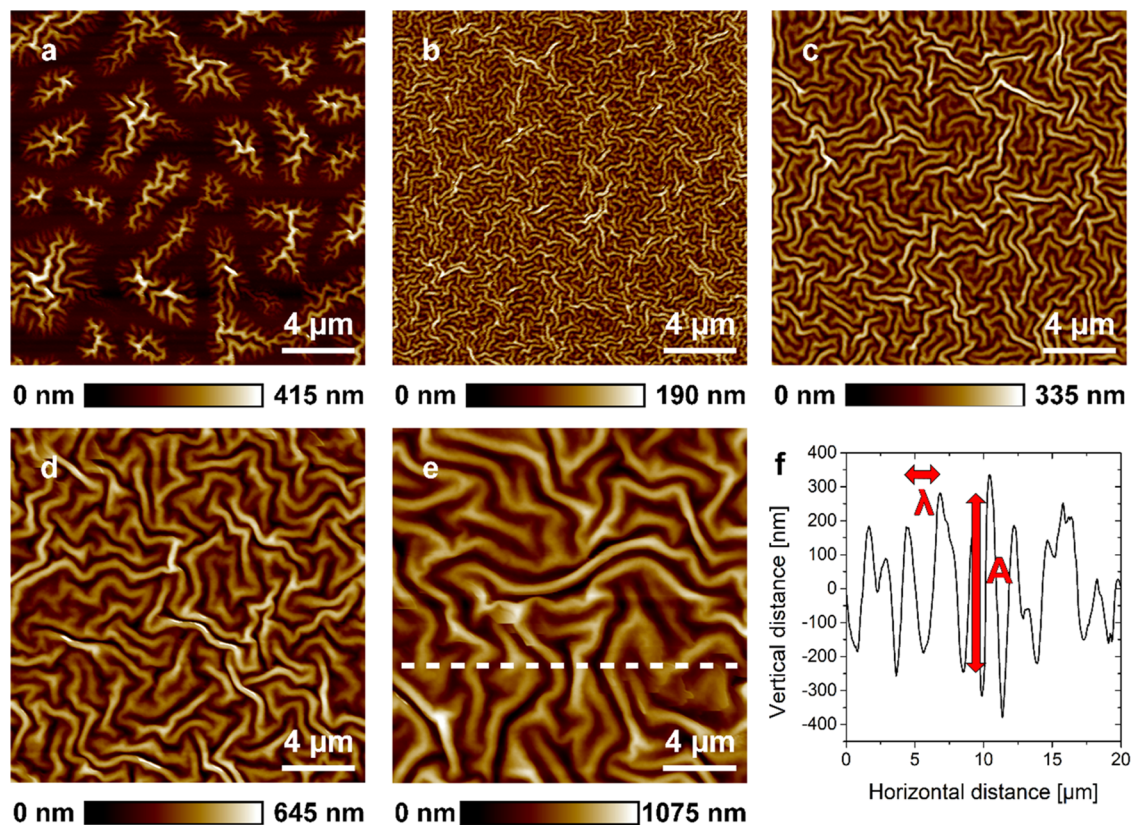


Figure 1. Topographic AFM images of PPF/50 nm thick Al bilayers for several PPF thicknesses: (a) 48 nm; (b) 95 nm; (c) 140 nm; (d) 285 nm; and (e) 425 nm, and its corresponding cross section (f).

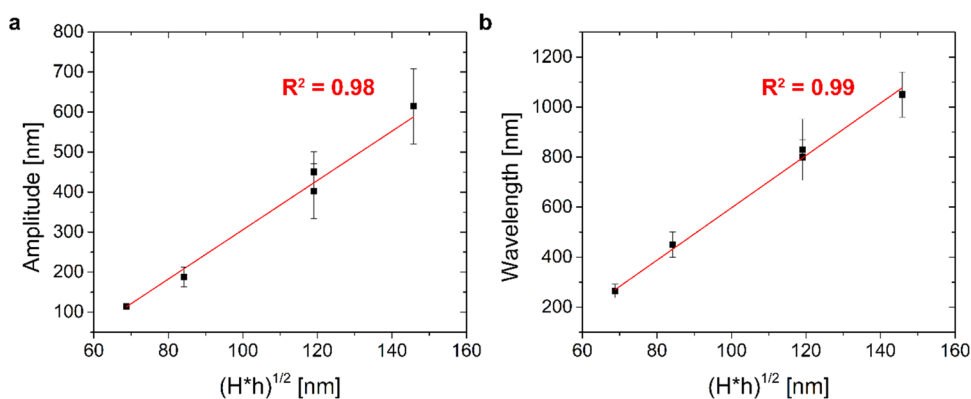


Figure 2. Evolution of (a) the amplitude and (b) wavelength of the wrinkles as a function of $(h \times H)^{1/2}$.

applied to the coil was fixed to 100 W; the other conditions being the same as described previously. The thickness of the layers was fixed at 100 nm.

The thickness of PPF was calibrated by atomic force microscopy (AFM) through the evaluation of the step height generated between the PPF surface and the Si substrate after a scratch was generated with a cutter blade.

Aluminum Deposition. The aluminum top layers (fixed at 50 nm) were deposited on propanethiol PPF by magnetron sputtering in a second chamber. The choice of this thickness is motivated by the lowest thickness considered for the bottom PPF (i.e., 48 nm). Indeed, for the wrinkling phenomenon to take place, the thickness of the top layer is usually lower or close to the bottom coating one.²³ The depositions were carried out with an aluminum target (5 cm in diameter) in an Ar atmosphere. The Ar flow rate and the working pressure have been fixed at 40 sccm and 7×10^{-3} Torr, respectively. A power of 100 W was applied to the target. A detailed description of the experimental setup can be found elsewhere.²⁴

Morphology Characterization. The topography of the samples has been recorded on images of 512 points \times 512 points by AFM. The AFM equipment is composed of a Bruker Multimode 8 microscope in tapping mode scanning configuration equipped with a Nanoscope III controller. Commercially available Silicon tips “RTESPA-190” (radius of curvature between 8 and 12 nm) provided by Bruker were used. The analysis of the AFM images was performed with the “Nanoscope Analysis” software. The average wavelength and amplitude have been determined through the section tool. At least 20 sections perpendicular to wrinkles located at different locations on the image have been performed. These hand measurements were consistent with the wavelength and amplitude evaluated using the power spectral density (PSD) and particle analysis tools, respectively. The topographic AFM images are presented as recorded only after considering plane-fitting processing.

Cross-sectional scanning electron microscopy imaging was carried out on an FEG-SEM Hitachi SU8020 microscope operating at 3 kV.

Chemical Composition Measurements. The PPF chemical composition was investigated by X-ray photoelectron spectroscopy (XPS). These analyses were performed using a PHI 5000 VersaProbe apparatus. A monochromated Al $K\alpha$ line (1486.6 eV) was used as a photon source. The atomic relative concentration of each element was calculated from peak areas considering the corresponding photoionization cross sections, the electron inelastic mean free path, and the transmission function of the spectrometer.

RESULTS AND DISCUSSION

In a first attempt, an aluminum coating (with a thickness fixed at 50 nm) is deposited on viscous PPF fluid, presenting a thickness varying from 48 to 425 nm. The corresponding AFM images of the layered system are depicted in Figure 1 illustrating the spontaneous occurrence of the wrinkling phenomenon. Interestingly, for a PPF thickness value of 48

nm, the wrinkles do not cover the entire surface but are dispersed in small asymmetric islands with the corresponding longest diameter of approximately 4–5 μm . The origin of this behavior will be discussed later.

As can be seen in Figure 1, starting from a PPF thickness of 95 nm, the wrinkles homogeneously cover the surface, and their dimensions vary with the thickness of the foundation layer. Indeed, both the wrinkle wavelength (i.e., peak-to-peak distances, λ) and amplitude (i.e., peak-to-valley distance, A) increase with the PPF thickness. λ evolves from 265 ± 27 to 1050 ± 90 nm, while A from 114.6 ± 6.6 to 614.5 ± 93.9 nm. For the sake of example, the PSD spectrum and particle analysis treatment of the topographic AFM image presented in Figure 1d are depicted in Figures S1 and S2, respectively.

It has already been demonstrated in the case of a thin metallic film deposited on a viscoelastic conventional polymeric fluid that the dimensions of the wrinkles evolve according to eq 1²⁵

$$\lambda \sim \frac{A}{2\sqrt{\delta_c}} \sim (h \times H)^{1/2} (E_M/E_P)^{1/6} \quad (1)$$

where δ_c is the compressive strain; h and H represent the thickness of the top and bottom layers, respectively; and E_M and E_P are the Young moduli of the metallic top layer and PPF bottom layer, respectively.

Then, the evolution of the amplitude and the wavelength of the wrinkles presented in Figure 1b–e are plotted as a function of $(h \times H)^{1/2}$ (Figure 2). Both the amplitude and the wavelength increase according to a $(h \times H)^{1/2}$ law ($R^2 > 0.9$), in line with eq 1 and the literature regarding conventional polymers.²⁵

Furthermore, according to eq 1, the slope of the linear relationship directly depends on the ratio between the elastic moduli of the bottom and top thin films. On this basis, considering a value of 85 GPa for E_M ,²⁶ E_P is estimated to be $\sim 7.5 \times 10^5$ Pa for the PPF bottom layer. It should be noted that the mechanical properties of this PPF have been previously investigated.²¹ However, only the viscous part of this sample could be evaluated (i.e., $\sim 10^6$ Pa s) as the technique employed to investigate its elastic modulus (i.e., PeakForce QNM measurements on AFM) was not suitable due to its viscous nature. Therefore, in addition to the control of the morphology of a material, the concept of the wrinkling process applied to plasma polymers can also be employed as a tool to probe their mechanical properties.²⁷ The elastic modulus value found here is consistent with our previous

results regarding the evolution of the mechanical properties of such coatings with the substrate temperature.²¹

Coming back to Figure 1a showing the dispersion of nanowrinkled domains on the surface, another major difference can be highlighted: the islands present higher structures in their center compared to their edges (i.e., 350 ± 50 vs 50 ± 20 nm). Vandeparre et al. have reported such typical morphologies in a hexagonal dotted pattern when an ultrathin layer of titanium (i.e., 15 nm) is deposited on thin (i.e., 40 nm) PS (polystyrene) film.²⁸ They demonstrated the non-negligible contribution of van der Waals (vdW) interactions between the metallic top layer and the Si substrate during the morphological reorganization process when the bottom layer thickness was lower than 100 nm. Considering the thickness of the PPF bottom layer in Figure 1a (i.e., 48 nm), it can be argued that vdW interactions partially drive the surface reorganization in islands by blowing the PPF layer in the localized area surrounded by an Al layer directly in contact with the Si substrate. Consequently, the wrinkling phenomenon following this reorganization leads to structured islands exhibiting higher wrinkles in the center than in the edges, as already observed by Yu et al. with magnetron-sputtered Cr deposited on silicon oil drops.²⁹

Based on the literature, as the top layer is supported by a viscoelastic fluid bottom material, the dimensions of the wrinkles are expected to evolve as a function of time following eq 2²⁵

$$\lambda \sim (h \times H)^{1/2} (E_M / \eta_p)^{1/6} t^{1/6} \quad (2)$$

where E_M represents the Young modulus (Pa) of the Al top layer, η_p the PPF viscosity (Pa s), and t the time (s).

Therefore, the bilayers described in Figure 1 have been imaged 100 days after their synthesis. An example of AFM images is presented in Figure 3a,b for the bilayer formed with a 140 nm thick PPF (i.e., Figure 1c) before and after the sample was stored in ambient air for 100 days. According to eq 1 and considering the aging duration (i.e., 100 days; i.e., 8.64×10^6 s), the wavelength and the amplitude of the wrinkles are expected to increase by a factor of ~ 2 .

However, the AFM images present similar topographies before and after aging. This observation is supported by the measurement of the wrinkle amplitude and the wavelength, which evolves from 194.1 ± 23.6 to 181.6 ± 21.7 nm and from 433.1 ± 40.1 to 409.1 ± 42.1 nm, respectively (Figure 3c). This phenomenon has been already observed by Yoo et al. regarding the deposition of a thin metallic layer on a thin viscoelastic fluid.³⁰ The stability of the wrinkles structure has been explained by a pinning phenomenon. During surface reorganization, the metallic layer approaches the substrate at a distance low enough for interacting with it to freeze the system, thus leading to wrinkles with dimensions stable over time. Consequently, cross-sectional scanning electron microscopy (SEM) analyses have been performed on Al/PPF bilayers to evaluate the distance between the Al layer and the Si substrate as presented in Figure 4.

In both cases, the metallic layer is at a distance typically ranging from several nanometers to 100 nm. Therefore, it can be reasonably argued that vdW interactions cannot be neglected, allowing to maintain wrinkle dimensions.^{28,31} Once the top layer is in contact with the substrate, the surface reorganization is frozen.

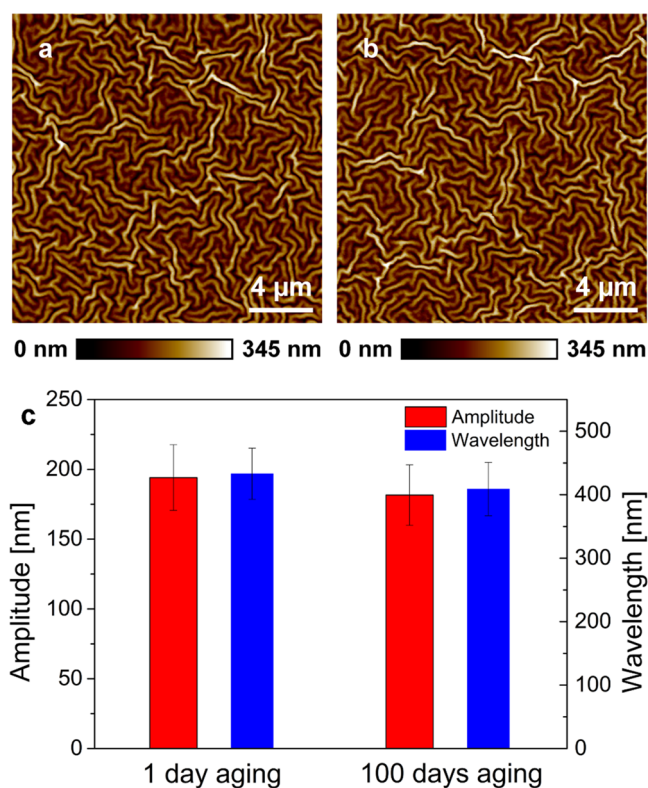


Figure 3. Topographic AFM images of 140 nm thick PPF/50 nm thick Al bilayer (a) 24 h after their synthesis and (b) 100 days after their synthesis. (c) Evolution of the amplitude and the wavelength of the wrinkles as a function of the aging duration.

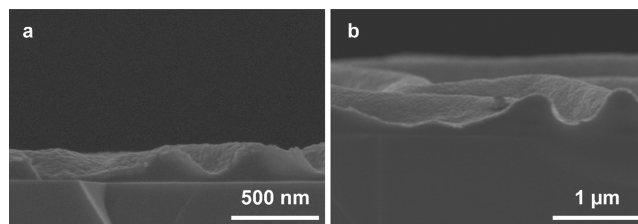


Figure 4. Cross-sectional SEM images of Al/PPF bilayers at different PPF thicknesses: (a) $H = 140$ nm and (b) $H = 425$ nm.

Finally, the wrinkled Al/PPF bilayers have been employed as patterns for further deposition of a functionalized PPF. To that purpose, plasma polymers (with a thickness of 100 nm) synthesized from two different precursors (i.e., propanethiol and allyl alcohol, referred to as SH-PPF_{100W} and OH-PPF_{100W}, respectively) have been deposited as a third layer on the SH-PPF/Al bilayers. The topography of the system before and after PPF deposition is presented in Figure 5.

Regardless of the initial dimensions of the wrinkles, similar topographies are observed before and after the upper PPF synthesis. Indeed, for the propanethiol-based third layer, λ and A evolve from 1343 ± 274 to 1361 ± 223 nm and from 707 ± 142 to 729 ± 81 nm, respectively (Figure 5a,b). Similarly, for the allyl alcohol-based third layer, λ (i.e., 515 ± 95 vs 484 ± 82 nm) and A (222 ± 22 vs 219 ± 22 nm) are not affected by the additional plasma polymer layer (Figure 5c,d).

The surface chemical composition before and after the deposition of the additional PPF is also investigated. As shown in Figure 6, for both precursors, the analysis of the XPS survey reveals that after the synthesis of the third layer, Al is no longer

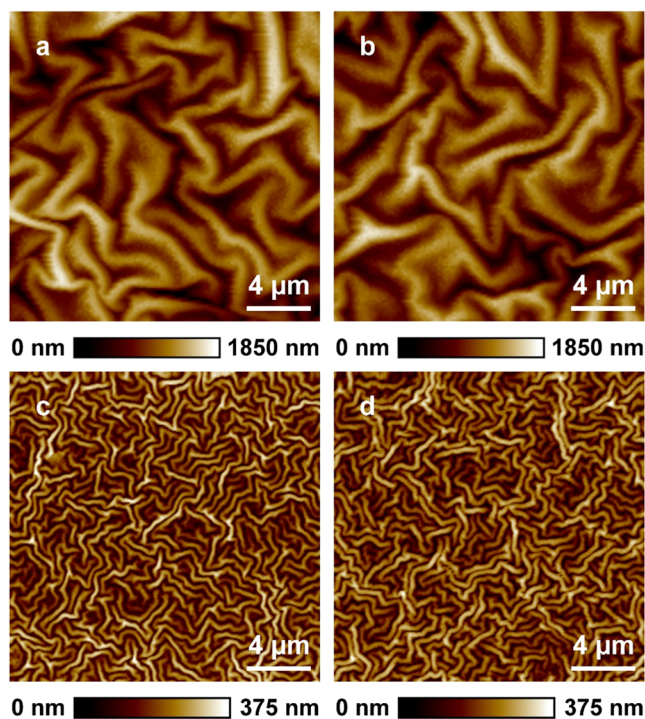


Figure 5. Topographic AFM images of (a) 570 nm thick PPF/50 nm thick Al bilayer, (b) 570 nm thick PPF/50 nm thick Al/100 nm thick SH-PPF_{100W} trilayer, (c) 140 nm thick PPF/50 nm thick Al bilayer, and (d) 140 nm thick PPF/50 nm thick Al/100 nm thick OH-PPF_{100W} trilayer.

identified. Only the elements of the top plasma polymer layer are present, indicating a homogeneous covering of the wrinkled pattern.

These data unambiguously demonstrate the availability to tune, on demand, the chemical composition of the surface without altering the topography of the patterns.

CONCLUSIONS

In this work, an innovative approach for the fabrication of nanostructured organic-based materials was established, combining the wrinkling phenomenon and the plasma polymerization process.

At first, the spontaneous morphological reorganization taking place in a bilayer system constituted by a highly viscous

liquid plasma polymer and Al as the foundation and top layers, respectively, was investigated. The dimensions of the wrinkles (i.e., their wavelength and their amplitude) were found to increase with the thickness of the polymeric layer according to a theoretical model established for conventional polymers, offering a remarkable control over the size of the nanostructure (i.e., λ evolves from 265 ± 27 to 1050 ± 90 nm, while A evolves from 114.6 ± 6.6 to 614.5 ± 93.9 nm). Interestingly, this correlation also enables us to determine the Young modulus of the plasma polymer layer, avoiding many difficulties inherent to methods to probe the mechanical properties of thin films. The dimensions of the wrinkles do not evolve with time, revealing the great stability of the structured surface. This is attributed to the low distance between the wrinkled top layer and the Si substrate (i.e., <100 nm), giving rise to a “pinning effect” freezing the morphology of the material, probably as a result of non-negligible vdW interactions.

At a further stage, the wrinkled material was employed as a pattern for the deposition of an additional functionalized plasma polymer. Regardless of the initial dimensions of the pattern, a conformal covering of the surface relief was achieved with tunable surface chemistry through an appropriate choice of precursor for the plasma polymerization process.

The attractiveness of the method herein developed lies in the ease of tailoring the nanoarchitecture as well as the chemical composition of the organic surface. This flexibility paves the way for the fabrication of a tailor-made organic-based material appealing for numerous applications, for instance in the biotechnology field (e.g., for driving the response of the material toward cell interaction). Furthermore, due to the good adhesion properties of plasma polymers, this strategy can potentially be applied to all kinds of substrates.

ASSOCIATED CONTENT

Supporting Information

The Supporting Information is available free of charge at <https://pubs.acs.org/doi/10.1021/acs.langmuir.3c01873>.

Typical PSD spectrum of a topographic AFM image (Figure S1). Typical “particle analysis” treatment of a topographic AFM image (Figure S2) (PDF)

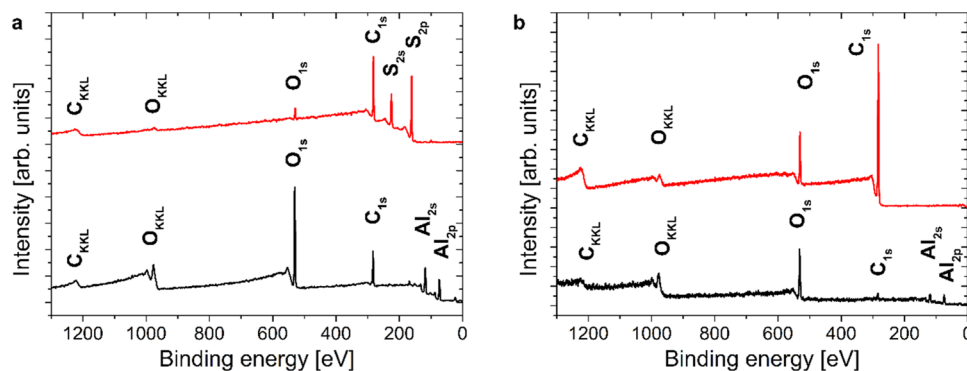


Figure 6. XPS survey spectra of (a) 570 nm thick PPF/50 nm thick Al bilayer (black line) and 570 nm thick PPF/50 nm thick Al/100 nm thick SH-PPF_{100W} trilayer (red line), (b) 140 nm thick PPF/50 nm thick Al bilayer (black line) and 140 nm thick PPF/50 nm thick Al/100 nm thick OH-PPF_{100W} trilayer (red line).

AUTHOR INFORMATION

Corresponding Author

Damien Thiry – *Chimie des Interactions Plasma-Surface (ChIPS), Institut Matériaux, Université de Mons, B-7000 Mons, Belgium*; orcid.org/0000-0001-6703-1512;
Email: Damien.Thiry@umons.ac.be

Authors

Nathan Vinx – *Chimie des Interactions Plasma-Surface (ChIPS), Institut Matériaux, Université de Mons, B-7000 Mons, Belgium*

David Tromont – *Chimie des Interactions Plasma-Surface (ChIPS), Institut Matériaux, Université de Mons, B-7000 Mons, Belgium*

Adrien Chauvin – *Chimie des Interactions Plasma-Surface (ChIPS), Institut Matériaux, Université de Mons, B-7000 Mons, Belgium*; orcid.org/0000-0003-1896-8776

Philippe Leclère – *Laboratoire de Physique des Nanomatériaux et Energie (LPNE), Institut Matériaux, Université de Mons, B-7000 Mons, Belgium*; orcid.org/0000-0002-5490-0608

Rony Snyders – *Chimie des Interactions Plasma-Surface (ChIPS), Institut Matériaux, Université de Mons, B-7000 Mons, Belgium; Materia Nova Research Center, B-7000 Mons, Belgium*

Complete contact information is available at:

<https://pubs.acs.org/10.1021/acs.langmuir.3c01873>

Author Contributions

The manuscript was written through contributions of all authors. All authors have given approval to the final version of the manuscript.

Notes

The authors declare no competing financial interest.

ACKNOWLEDGMENTS

N.V. would like to thank Prof. Pascal Damman (Umons, Belgium) for the fruitful discussions related to this work.

ABBREVIATIONS

PPF, plasma polymer film; AFM, atomic force microscopy; XPS, X-ray photoelectron spectroscopy; PSD, power spectral density

REFERENCES

- (1) Cools, P.; Astoreca, L.; Esbah Tabaei, P. S.; Thukkaram, M.; De Smet, H.; Morent, R.; De Geyter, N. Surface treatment of polymers by plasma. *Surf. Modif. Polym.: Methods Appl.* **2019**, 31–65.
- (2) Thiry, D.; Reniers, F.; Snyders, R. A Joint Mechanistic Description of Plasma Polymers Synthesized at Low and Atmospheric Pressure. *Surf. Modif. Polym.: Methods Appl.* **2019**, 67–106.
- (3) Snyders, R.; Hegemann, D.; Thiry, D.; Zabeida, O.; Klemberg-Sapieha, J. E.; Martinu, L. Foundations of plasma enhanced chemical vapor deposition of functional coatings. *Plasma Sources Sci. Technol.* **2023**, 32, No. 074001.
- (4) Biederman, H. *Plasma Polymer Films*; World Scientific, 2004.
- (5) Inagaki, N. *Plasma Surface Modification and Plasma Polymerization*; CRC Press, 1996.
- (6) Yasuda, H.; Matsuzawa, Y. Economical Advantages of Low-Pressure Plasma Polymerization Coating. *Plasma Processes Polym.* **2005**, 2 (6), 507–512.
- (7) Asadian, M.; Onyshchenko, I.; Thiry, D.; Cools, P.; Declercq, H.; Snyders, R.; Morent, R.; De Geyter, N. Thiolation of polycaprolactone (PCL) nanofibers by inductively coupled plasma

(ICP) polymerization: Physical, chemical and biological properties. *Appl. Surf. Sci.* **2019**, 479, 942–952.

(8) Bitar, R.; Cools, P.; De Geyter, N.; Morent, R. Acrylic acid plasma polymerization for biomedical use. *Appl. Surf. Sci.* **2018**, 448, 168–185.

(9) Liang, H.; Panepinto, A.; Prince, L.; Olivier, M.; Cossement, D.; Bousser, E.; Geng, X.; Li, W.; Chen, M.; Snyders, R.; Thiry, D. Study of the synthesis of C: H coating by PECVD for protecting Mg-based nano-objects. *Plasma Processes Polym.* **2020**, 17 (11), No. 2000083.

(10) Grundmeier, G.; Thiemann, P.; Carpentier, J.; Barranco, V. Tailored thin plasma polymers for the corrosion protection of metals. *Surf. Coat. Technol.* **2003**, 174–175, 996–1001.

(11) Jacob, M. V.; Olsen, N. S.; Anderson, L. J.; Bazaka, K.; Shanks, R. A. Plasma polymerised thin films for flexible electronic applications. *Thin Solid Films* **2013**, 546, 167–170.

(12) Thiry, D.; Vinx, N.; Damman, P.; Aparicio, F. J.; Tessier, P. Y.; Moerman, D.; Leclère, P.; Godfroid, T.; Desprez, S.; Snyders, R. The wrinkling concept applied to plasma-deposited polymer-like thin films: A promising method for the fabrication of flexible electrodes. *Plasma Process. Polym.* **2020**, 17 (9), No. 2000119.

(13) Iqbal, M.; Dinh, D. K.; Abbas, Q.; Imran, M.; Sattar, H.; Ul Ahmad, A. Controlled surface wettability by plasma polymer surface modification. *Surfaces* **2019**, 2 (2), 349–371.

(14) Artemenko, A.; Kozak, H.; Biederman, H.; Choukourov, A.; Kromka, A. Amination of NCD films for possible application in biosensing. *Plasma Processes Polym.* **2015**, 12 (4), 336–346.

(15) Hegemann, D.; Indutnyi, I.; Zajíčková, L.; Makhneva, E.; Farka, Z.; Ushenin, Y.; Vandenbosche, M. Stable, nanometer-thick oxygen-containing plasma polymer films suited for enhanced biosensing. *Plasma Processes Polym.* **2018**, 15 (11), No. 1800090.

(16) Thiry, D.; Chauvin, A.; El Mel, A. A.; Cardinaud, C.; Hamon, J.; Gautron, E.; Stephant, N.; Granier, A.; Tessier, P. Y. Tailoring the chemistry and the nano-architecture of organic thin films using cold plasma processes. *Plasma Processes Polym.* **2017**, 14 (11), No. 1700042.

(17) Soppera, O.; Dirani, A.; Ponche, A.; Roucoules, V. Nanopatterning of plasma polymer reactive surfaces by DUV interferometry. *Nanotechnology* **2008**, 19 (39), No. 395304.

(18) Brétagnot, F.; Valsesia, A.; Sasaki, T.; Ceccone, G.; Colpo, P.; Rossi, F. Direct nanopatterning of 3D chemically active structures for biological applications. *Adv. Mater.* **2007**, 19 (15), No. 1947.

(19) Goessl, A.; Bowen-Pope, D. F.; Hoffman, A. S. Control of shape and size of vascular smooth muscle cells in vitro by plasma lithography. *J. Biomed. Mater. Res.: Off. J. Soc. Biomater., Jpn. Soc. Biomater., Aust. Soc. Biomater. Korean Soc. Biomater.* **2001**, 57 (1), 15–24.

(20) Kylián, O.; Choukourov, A.; Biederman, H. Nanostructured plasma polymers. *Thin Solid Films* **2013**, 548, 1–17.

(21) Vinx, N.; Damman, P.; Leclère, P.; Bresson, B.; Fretigny, C.; Poleunis, C.; Delcorte, A.; Cossement, D.; Snyders, R.; Thiry, D. Investigating the relationship between the mechanical properties of plasma polymer-like thin films and their glass transition temperature. *Soft Matter* **2021**, 17 (44), 10032–10041.

(22) Thiry, D.; Britun, N.; Konstantinidis, S.; Dauchot, J.-P.; Guillaume, M.; Cornil, J.; Snyders, R. Experimental and theoretical study of the effect of the inductive-to-capacitive transition in propanethiol plasma polymer chemistry. *J. Phys. Chem. C* **2013**, 117 (19), 9843–9851.

(23) Rodríguez-Hernández, J. Wrinkled interfaces: taking advantage of surface instabilities to pattern polymer surfaces. *Prog. Polym. Sci.* **2015**, 42, 1–41.

(24) Nouvellon, C.; Belchi, R.; Libralesso, L.; Douhéret, O.; Lazzaroni, R.; Snyders, R.; Thiry, D. WC/C: H films synthesized by an hybrid reactive magnetron sputtering/Plasma Enhanced Chemical Vapor Deposition process: An alternative to Cr (VI) based hard chromium plating. *Thin Solid Films* **2017**, 630, 79–85.

(25) Vandeparre, H.; Gabriele, S.; Brau, F.; Gay, C.; Parker, K. K.; Damman, P. Hierarchical wrinkling patterns. *Soft Matter* **2010**, 6 (22), 5751–5756.

(26) Saha, R.; Nix, W. D. Effects of the substrate on the determination of thin film mechanical properties by nanoindentation. *Acta Mater.* **2002**, *50* (1), 23–38.

(27) Chung, J. Y.; Nolte, A. J.; Stafford, C. M. Surface wrinkling: a versatile platform for measuring thin-film properties. *Adv. Mater.* **2011**, *23* (3), 349–368.

(28) Vandeparre, H.; Desbief, S.; Lazzaroni, R.; Gay, C.; Damman, P. Confined wrinkling: impact on pattern morphology and periodicity. *Soft Matter* **2011**, *7* (15), 6878–6882.

(29) Yu, S.-J.; Zhang, Y.-J.; Zhou, H.; Chen, M.-G.; Zhang, X.-F.; Jiao, Z.-W.; Si, P.-Z. Spontaneous formation of hierarchical wrinkles in Cr films deposited on silicone oil drops with constrained edges. *Phys. Rev. E* **2013**, *88* (4), No. 042401.

(30) Yoo, P. J.; Lee, H. H. Morphological diagram for metal/polymer bilayer wrinkling: Influence of thermomechanical properties of polymer layer. *Macromolecules* **2005**, *38* (7), 2820–2831.

(31) Kang, S. H.; Na, J.-H.; Moon, S. N.; Lee, W. I.; Yoo, P. J.; Lee, S.-D. Self-organized anisotropic wrinkling of molecularly aligned liquid crystalline polymer. *Langmuir* **2012**, *28* (7), 3576–3582.